original article

Annals of Oncology 19: 1860–1869, 2008
doi:10.1093/annonc/mdn406
Published online 17 July 2008

Synergic antitumoral effect of an IGF-IR inhibitor and trastuzumab on HER2-overexpressing breast cancer cells

A. Esparís-Ogando[1†], A. Ocaña[1,2†], R. Rodríguez-Barrueco[1†], L. Ferreira[1], J. Borges[1] & A. Pandiella[1*]

[1]*Instituto de Biología Molecular y Celular del Cáncer, CSIC-Universidad de Salamanca;* [2]*Servicio de Oncología Médica, Complejo Hospitalario Universitario de Albacete, Spain*

Received 4 March 2008; revised 30 May 2008; accepted 2 June 2008

Background: Receptor tyrosine kinases play an important role in breast cancer. One of them, the type I insulin-like growth factor, has been linked to resistance to trastuzumab (Herceptin), an agent that targets human epidermal growth factor receptor 2. Here, we show that the insulin-like growth factor-I receptor (IGF-IR) antagonist NVP-AEW541 inhibits proliferation of breast cancer cells and synergizes with trastuzumab.

Patients and methods: Patient samples and breast cancer cell lines were evaluated for IGF-IR expression or activation by western blotting. 1-(4,5-Dimethylthiazol-2-yl)-3,5-diphenylformazan (MTT) uptake assays and Annexin V staining were used for the analyses of cell proliferation/apoptosis. Biochemical and genomic studies were carried out to gain insights into the mechanism of action of NVP-AEW541.

Results: The IGF-IR was expressed above normal levels in a number of breast cancer samples. Activation of this receptor was inhibited by NVP-AEW541 that also decreased cell proliferation and increased apoptosis. NVP-AEW541 decreased the amount of pAkt and increased the level of p27. Combination studies with several drugs used in the breast cancer clinic showed that NVP-AEW541 synergistically increased the action of trastuzumab.

Conclusions: Our results show the anti-breast cancer action of NVP-AEW541 and support the clinical development of anti-IGF-IR agents, especially in combination with trastuzumab.

Key words: breast cancer, IGF-IR, trastuzumab

introduction

Receptor tyrosine kinases (RTKs) have been associated with the development/progression of different types of cancer [1, 2]. In breast cancer, overexpression of one of these RTKs, termed ErbB2/human epidermal growth factor receptor 2 (HER2), occurs approximately in 25% of patients and is associated with shorter survival [3, 4]. These findings led to the development of agents that target HER2. One of these compounds is trastuzumab, a monoclonal antibody that acts on the extracellular domain of HER2 [5, 6]. In HER2-overexpressing breast cancer tumors, treatment with trastuzumab increases survival in metastatic and early-stage breast cancer [7, 8].

In spite of its effectiveness in breast cancer, a substantial number of HER2-positive patients do not respond to trastuzumab or relapse in a short period of time. This resistance to trastuzumab has been attributed to various mechanisms, including phosphatase and tensin homolog (PTEN) inactivation [9], the presence of HER2-truncated forms [10], or the activation of other tyrosine kinase receptors such as the insulin-like growth factor-I receptor (IGF-IR) [11]. IGF-IR is a heterotetrameric transmembrane tyrosine kinase receptor that is widely expressed in normal human tissues [12, 13]. After binding to IGF-I, the receptor phosphorylates the insulin receptor substrate 1 (IRS-1) that is responsible for mediating the activation of multiple downstream signaling networks, including the phosphatidylinositol-3-kinase or the Ras/Raf/mitogen-activated protein kinase pathways. Activation of these signaling pathways leads to stimulation of cell cycle progression and resistance to cell death. In addition, a second adaptor protein, termed IRS-2, is also activated by the IGF-IR and participates in mediating motility signals.

Increased levels of IGF-I in the blood are associated with an increased risk of breast cancer [14], and overexpression of IGF-IR and its ligands has been associated to the development and maintenance of breast cancer [13,15–17]. In addition, ligand-induced stimulation of the IGF-IR inhibits the action of trastuzumab [11]. These facts led to efforts aimed at developing treatments to decrease IGF-IR function to be used

Correspondence to: Dr A. Pandiella, Instituto de Biología Molecular y Celular del Cáncer, Campus Miguel de Unamuno, 37007-Salamanca, Spain. Tel/Fax: +34-923-294815; E-mail: atanasio@usal.es

†These authors contributed equally to the work.

directly to treat breast cancer and to help in the reversion of trastuzumab resistance. During the last years, several types of agents that target the IGF-IR have been developed, including small tyrosine kinase inhibitors, monoclonal antibodies, or IGF-I-binding proteins. Although monoclonal antibodies are in clinical development [18], some studies indicate that some of these antibodies can also down-regulate the insulin receptor and may provoke metabolic disorders such as 'hyperglycemia' [19, 20]. Furthermore, monoclonal antibodies or other protein antagonists have the inconvenience of parenteral administration that requires treatment of the patient at the clinic. To circumvent these problems, specific IGF-IR small molecule tyrosine kinase inhibitors that do not affect glucose metabolism are in clinical development. One of these compounds, the pyrrolopyrimidine derivative NVP-ADW742, has demonstrated potent antitumor activity against several tumoral cells [21]. A more recently developed analog, termed NVP-AEW541, has shown a 27-fold inhibitory selectivity for IGF-IR with respect to the insulin receptor and is more specific than NVP-ADW742 [20, 22]. Moreover, NVP-AEW541 prevented the growth of different tumoral cell lines *in vitro* and *in vivo* [20, 22, 23]. However, its action on breast cancer cells has not been explored in detail.

Given the importance of the IGF-IR in breast cancer and the potential clinical benefit of agents that target this signaling pathway, we explored the action of NVP-AEW541 on breast cancer cells. Here, we show that IGF-IR overexpression is frequent in patients with breast cancer. Studies using cell lines showed that NVP-AEW541 reduces proliferation and acts synergistically with trastuzumab in restricting proliferation of breast cancer cells. This latter finding is of particular importance as it opens the possibility of combining anti-IGF-IR therapies such as NVP-AEW541 with trastuzumab for the more efficient treatment of trastuzumab-sensitive breast cancers.

materials and methods

reagents and immunochemicals

NVP-AEW541 was from Novartis Pharma (Basel, Switzerland). Other generic chemicals, as well as docetaxel and vincristine were from Sigma Chemical Co. (St. Louis, MO), Roche Biochemicals (Indianapolis, IN), or Merck (Darmstadt, Germany). IGF-I was from Strathmann (Hamburg, Germany). Trastuzumab and Neuregulin (NRG) were a generous gift of Dr Mark X. Sliwkowski (Genentech, San Francisco, CA). The anti-phosphotyrosine, anti-glyceraldehyde-3-phosphate dehydrogenase (GAPDH), anti-cyclin D1, the rabbit polyclonal anti-p21, anti-p27, anti-IGF-IR, anti-Cdk2, and anti-cyclin D3 were from Santa Cruz Biotechnology (Sta. Cruz, CA). The anti-phospho-IGF-IR antibody used for western blotting was from Cell Signalling (Beverly, MA). We observed that the latter antibody also reacts with anti-pHER2 in western blots (data not shown). Horseradish peroxidase conjugates of anti-rabbit and anti-mouse immunoglobulin G were from Bio-Rad Laboratories (Cambridge, MA). The anti-pAkt Ser^{473} antibody was generated against the sequence RPHFPQFpS^{473}YSAS.

cell culture, immunoprecipitation, and western blotting

All cell lines were cultured at 37°C in a humidified 5% CO_2/95% air atmosphere. Cells were grown in Dulbecco's modified Eagle's medium containing high glucose (4500 mg/l) and antibiotics (penicillin 100 units/ml, streptomycin 100 μg/ml) and supplemented with 10% foetal bovine serum. Immunoprecipitation and western blotting were carried out as described [24]. Conditions for the analysis of the cell cycle and proliferation in breast cancer cells have been reported [25].

apoptosis analyses

For apoptosis analyses, trypsinized cells were washed twice with cold phosphate-buffered saline (PBS) and then resuspended in binding buffer (10 mM Hepes, pH 7.4, 140 mM NaCl, 2.5 mM $CaCl_2$) at a concentration of 1×10^6 cells/ml. In total, 100 000 cells were incubated for 15 min in the dark with 5 μl of Annexin V–fluorescein isothiocyanate (FITC) (BD Biosciences) and 10 μl of propidium iodide (5 μg/ml, final concentration). Finally, 400 μl of binding buffer was added. Apoptosis analyses were carried out on a FACSCalibur machine using the CellQuest software (BD Biosciences, Franklin Lakes, NJ).

Mitochondrial membrane potential was analyzed by the incorporation of tetramethylrhodamine ethyl ester (TMRE). In total, 220 000 BT474 cells were plated in 60-mm dishes, allowed to attach during 24 h and treated with different doses of NVP-AEW541 for 72 h. TMRE (1 μM) was added to the plate for 30 min, and then cells were trypsinized and resuspended in 500 μl of PBS before fluorescence quantification on a FACSCalibur cytometer (BD Biosciences, Franklin, NJ).

analyses of synergism by the CalcuSyn program

In order to determine whether the combination of NVP-AEW541 and trastuzumab was additive, antagonist, or synergistic, we used the CalcuSyn software program (Biosoft, Ferguson, MO). This program allows the calculation of the combination index (CI) following the algorithm of Chou and Talalay [26]. CI values <1.0 indicate synergism, CI = 1 indicates an additive effect, whereas values >1 correspond to antagonism. CIs from two different experiments were generated with the CalcuSyn software for each combination and graphically represented as the mean ± standard deviation.

microarray RNA analyses

Total RNA was extracted and purified with RNeasy Mini Kit (Qiagen, CA). Double-stranded complementary DNA and afterwards biotinylated complementary RNA were synthesized using a T7-polyT primer and the BioArray RNA labeling kit (Enzo, NY), respectively. The labeled RNA was then fragmented and hybridized according to Affymetrix protocols to HU-133 Plus 2.0 oligonucleotide arrays (Affymetrix, CA). The expression values for each probe set were calculated using the dChip 2006 software. All samples had a scaling factor lower than two-fold and a 3′–5′ of GAPDH probe set <1.5. Gene expression levels were transformed to base two logarithms. A median normalization approach was applied.

results

expression of IGF-IR in patient samples and human breast cancer cell lines

We evaluated the presence of the IGF-IR in 22 samples from breast cancer patients, using as a control normal glandular breast tissue (Figure 1A). The anti-IGF-IR antibody used identified a 97-kDa form, together with two additional bands of 180 and 200 kDa (asterisks in Figure 1A). The 97-kDa band migrated with the expected molecular mass of the β chain of the IGF-IR, while the upper molecular mass forms may correspond to the unprocessed immature receptor. Levels of IGF-IR substantially higher than those present in control breast tissue were present in nine (40%) of the samples. Amounts of IGF-IR analogous to those of control normal breast epithelium were observed in eight (37%) samples.

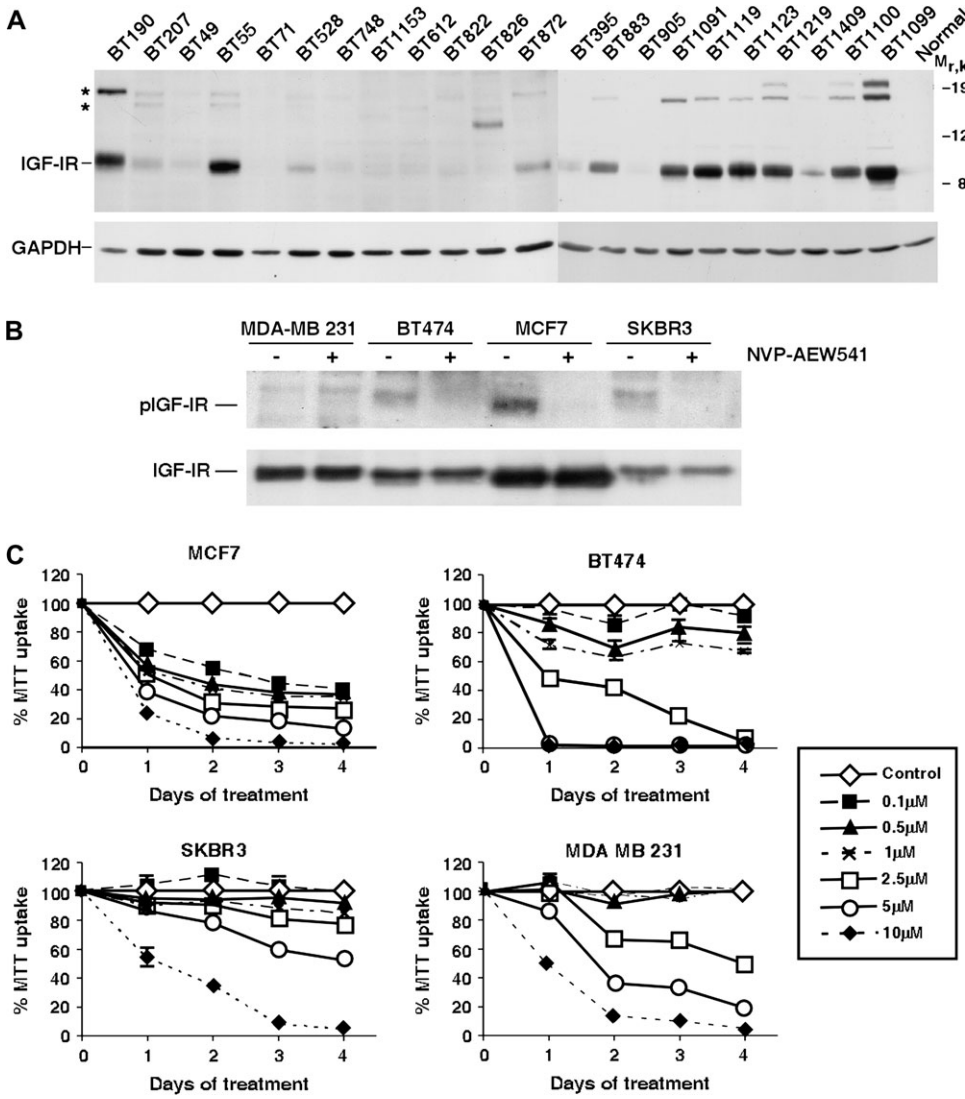

Figure 1. Expression of insulin-like growth factor-I receptor (IGF-IR) in patient samples and characterization of its pathway in breast cancer cells. (A) Expression of IGF-IR in breast cancer patient samples. In total, 80 μg of lysates from breast tumors and normal tissue was analyzed by western blotting with an anti-IGF-IR antibody. Asterisks indicate higher molecular weight bands reactive with the antibody. (B) NVP-AEW541 (1 μM) was added to the indicated cell lines and p-IGF-IR or IGF-IR analyzed by immunoprecipitation with the anti-IGF-IR, followed by western with anti-IGF-IR or anti-PY antibodies. (C) Dose-dependent action of NVP-AEW541 on breast cancer cells. In total, 20 000 cells were cultured in 24-well plates 24 h before adding NVP-AEW541. MTT uptakes were determined at the indicated days of treatment. The results show the mean ± standard deviation of quadruplicates of an experiment that was repeated three times.

action of NVP-AEW541 on breast cancer cell lines

To explore the action of NVP-AEW541 in breast cancer, we used several cell lines representative of distinct molecular pathological situations. Two of them, BT474 and SKBR3, are frequently used as model cell lines of HER2 overexpression, while the MCF7 cell line contains a low to normal HER2 level [27]. MDA-MB231 cells are representative of the triple-negative genotype [28], characterized by the absence of hormonal receptors and HER2 amplification. The different breast cancer cell lines were treated with a fixed dose of the drug, and tyrosine phosphorylation IGF-IR was analyzed by western blotting. On sufficiently long exposure times, and upon enrichment of the IGF-IR by immunoprecipitation, resting tyrosine phosphorylation of the IGF-IR was observed in BT474, MCF7, and SKBR3 cells (Figure 1B). Addition of NVP-AEW541 inhibited the constitutive tyrosine phosphorylation of the IGF-IR in MCF7, BT474, and SKBR3 cells. No resting level of tyrosine-phosphorylated IGF-IR was detected in MDA-MB231 cells.

We evaluated the anti-proliferative activity of NVP-AEW541 in the four breast cancer cell lines. In MCF7 cells, treatment with NVP-AEW541 inhibited the MTT absorbance of these cells in a dose-dependent manner (Figure 1C). In BT474 cells, the growth inhibitory effect of NVP-AEW541 was less marked than in MCF7 cells for doses up to 2.5 μM. SKBR3 cells that express much lower IGF-IR levels than the other cell lines analyzed were less sensitive to the action of NVP-AEW541, and higher doses of the compound were required to inhibit their

growth. Interestingly, NVP-AEW541 also decreased MTT metabolization in the triple-negative cell line MDA-MB231.

The decrease in the MTT uptake could be caused by reduced proliferation or cell death. To investigate the potential contribution of these biological responses to the action of NVP-AEW541, we carried out propidium iodide staining followed by fluorescence-activated cell sorter analysis of BT474 cells. Addition of NVP-AEW541 provoked a dose-dependent increase in the G_0/G_1 phases and a decrease in the G_2/M and S phases (Figure 2A). Biochemical evaluation of the action of NVP-AEW541 on signaling routes and proteins involved in the control of cell cycle progression was also carried out. NVP-AEW541 provoked an increase in p27, together with a decrease in p21 (Figure 2B). No significant changes were observed in the amounts of cyclin-dependent kinase 2 (CDK2) or cyclin D1. NVP-AEW541 decreased pAkt levels.

Analyses of apoptotic cell death by Annexin V–FITC staining indicated that NVP-AEW541 provoked an increase in BT474 apoptotic cells (Figure 2C). In parallel, we also measured the mitochondrial membrane potential, using TMRE staining (Figure 2D). NVP-AEW541 significantly affected the mitochondrial membrane potential.

synergistic effect of NVP-AEW541 in combination with trastuzumab

We next evaluated the potential synergistic effect of NVP-AEW541 and trastuzumab on breast cancer cells. In BT474 and SKBR3 cells, treatment with this drug combination resulted in a significant inhibitory effect when compared with the drug being added alone (Figure 3A). In MCF7 cells, that are insensitive to trastuzumab [29], addition of both compounds did not significantly increase the effect of the individual drug treatments. The increased efficiency of the combined treatment in BT474 cells was already evidenced within 2 days and persisted for as long as 8 days (Figure 3B). To assess whether this potentiation effect was synergistic or additive, we used the CI algorithm of Chou and Talalay. In BT474 cells, and as shown in Figure 3C, a clear synergistic effect of NVP-AEW541 and trastuzumab was obtained at 1, 1.5, and 2 μM doses of NVP-AEW541 when combined with a fixed and maximal dose (10 nM) of trastuzumab.

We also explored whether NVP-AEW541 could potentiate the action of other compounds commonly used in the treatment of breast cancer. To this end, we first evaluated the antitumoral effect of a taxane (docetaxel) and a vinca

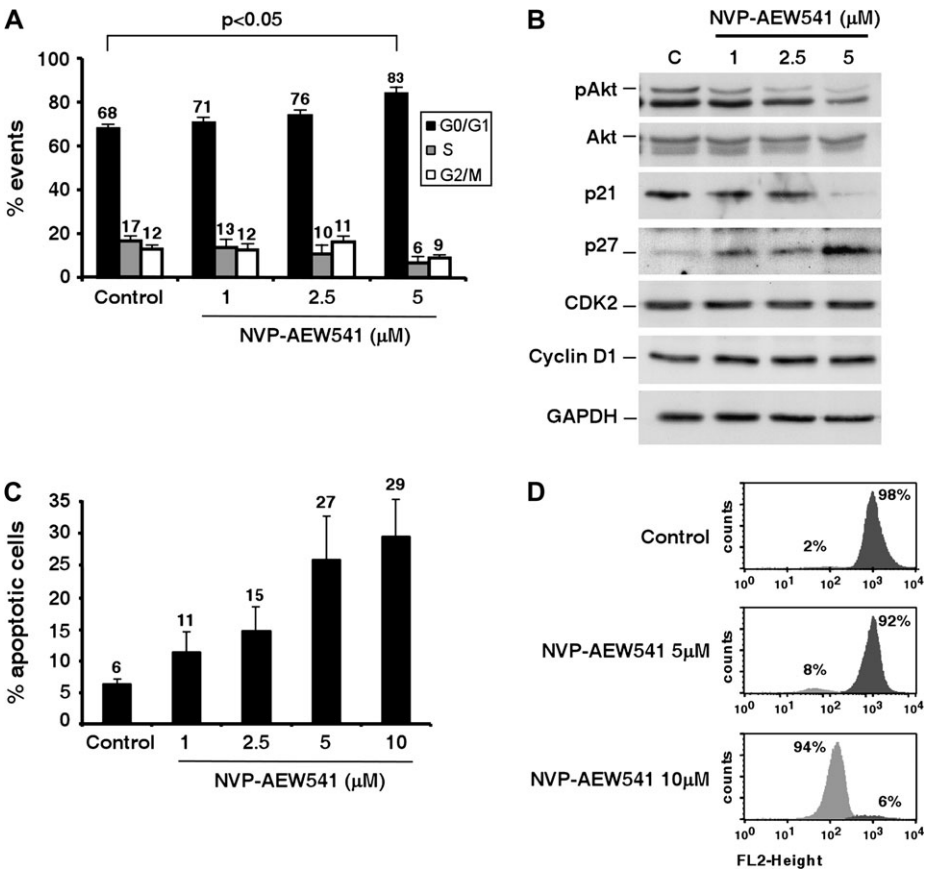

Figure 2. Effect of NVP-AEW541 on cell cycle and apoptosis on breast cancer cells. (A) Cell cycle profiling of BT474 cells after treatment with different doses of NVP-AEW541 for 72 h. Numbers above bars indicate the percentage of cells in each phase. The data are representative of three experiments. Statistic analyses were carried out using the non-parametric Kruskal–Wallis test. (B) Analysis of the action of NVP-AEW541 on proteins involved in cell cycle progression. BT474 cells were treated for 72 h with NVP-AEW541, and expression of proteins related with cell cycle was analyzed by western blot. (C) Measurement of Annexin V staining of BT474 cells treated with NVP-AEW541 for 72 h. The data shown are representative of three experiments. (D) Analyses of the mitochondrial membrane potential in BT474 cells treated with NVP-AEW541 for 72 h.

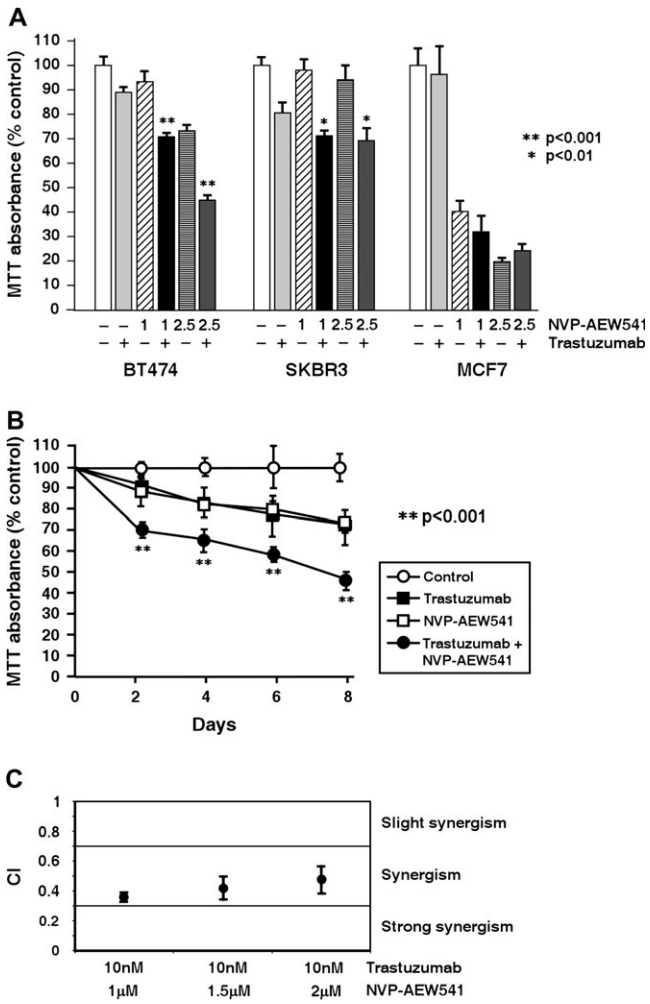

Figure 3. Synergistic effect of NVP-AEW541 in combination with trastuzumab. (A) Action, measured by MTT uptake, of the combination of different doses of NVP-AEW541 with trastuzumab (10 nM) on breast cancer cells. The asterisks indicate a $P < 0.001$ or a $P < 0.01$ of the effect of the double combination with respect to the action of the individual treatments. (B) Sustained potentiation effect of NVP-AEW541 (2.5 μM) in combination with trastuzumab (10 nM) in BT474 cells. The asterisks indicate a $P < 0.001$ of the effect of the double combination with respect to the action of the individual treatments, at each corresponding time. (C) Effect of the combination on BT474 cells using the CalcuSyn software and representing the combination index (CI). The graphic represents the mean ± standard deviation of the CI from the results of two independent experiments.

alkaloid (vincristine) on BT474 cells, to select for an adequate dose to be combined with NVP-AEW541. Both compounds had a potent anti-proliferative/proapoptotic effect on BT474 cells both at 3 or at 6 days of treatment, with IC_{50} values of 5 nM for docetaxel and 0.5 nM for vincristine (Figure 4A). The quadruple combination of these agents (trastuzumab + docetaxel + vincristine + NVP-AEW541) was more efficient than the addition of these compounds in double or triple combinations (Figure 4B, and data not shown).

To gain insights into the mechanism of potentiation of the action of trastuzumab by NVP-AEW541, we carried out biochemical and genomic profiling studies. For these experiments, BT474 cells were treated with a saturating dose of trastuzumab, and a suboptimal dose of NVP-AEW541 for 3 or 6 days, and then MTT assays carried out to check efficient synergic action of both compounds. In parallel, cell lysates were prepared from sister cultures, and protein and messenger RNA (mRNA) extracted. Biochemical studies indicated that the combined treatment decreased the levels of pAkt and increased p27 more profoundly than either treatment alone. The levels of cyclin D1 and cyclin D3 remained unchanged, while the amount of p21 slightly decreased by the single or the combined treatments (Figure 4C and data not shown).

Microarray studies identified 119 mRNAs selectively up- or down-regulated by the combined treatment. Neither the amount of these mRNAs was also modified by trastuzumab or NVP-AEW541 nor their levels were substantially higher or lower when compared with the individual treatments (Table 1). The mostly up-regulated mRNA corresponded to the prolactin-induced protein (PIP), and the mostly down-regulated mRNA corresponded to fascin homolog 1. In addition, p8, a protein recently described to be involved in the control of apoptosis, was up-regulated [30]. The increases in the mRNA for PIP or p8 proteins were also verified by quantitative RT-PCR (Figure 4D). Some mRNAs related to cell cycle progression, such as E2F4, E2F5, TFDP1, or cyclin G, were also specifically modified by the combined treatment. A significant number of mRNAs related to the control of proteolytic processes, including proteases and protease inhibitors, as well as mRNAs coding for proteins involved in metabolic regulation were also controlled by the combined treatment.

discussion

The present study was initiated with the purpose of evaluating the action of the IGF-IR antagonist NVP-AEW541 on breast cancer cells. The rationale for this study was on the basis of several data that linked the IGF-IR to tumor generation/progression [13, 15], together with the favorable antitumoral action of protein antagonists of the IGF-IR system [20, 31]. Furthermore, as IGF-IR has been associated to trastuzumab resistance, the combination of an anti-IGF-IR antagonist with trastuzumab could help to overcome resistance to the latter [11, 32].

We analyzed the presence of IGF-IR in breast cancer tumors from patients by western blotting. Overexpression of IGF-IR was observed in 40% of the samples studied. It is important to mention that normal breast epithelial tissue expresses low levels of IGF-IR (Figure 1A and [13]). This increased expression, together with the demonstrated role of IGF-IR in stimulating breast cancer cell proliferation, positions IGF-IR as a candidate target for breast cancer treatment. In support of the latter are our *in vitro* data with NVP-AEW541, as well as data from other groups using alternative anti-IGF-IR strategies [11, 31, 32]. In our experimental setting, NVP-AEW541 substantially decreased MTT uptake of all four breast cancer cell lines studied. It should be mentioned that these cell lines represent prototypic models of three phenotypically different molecular situations: the estrogen receptor positive, but HER2-negative status

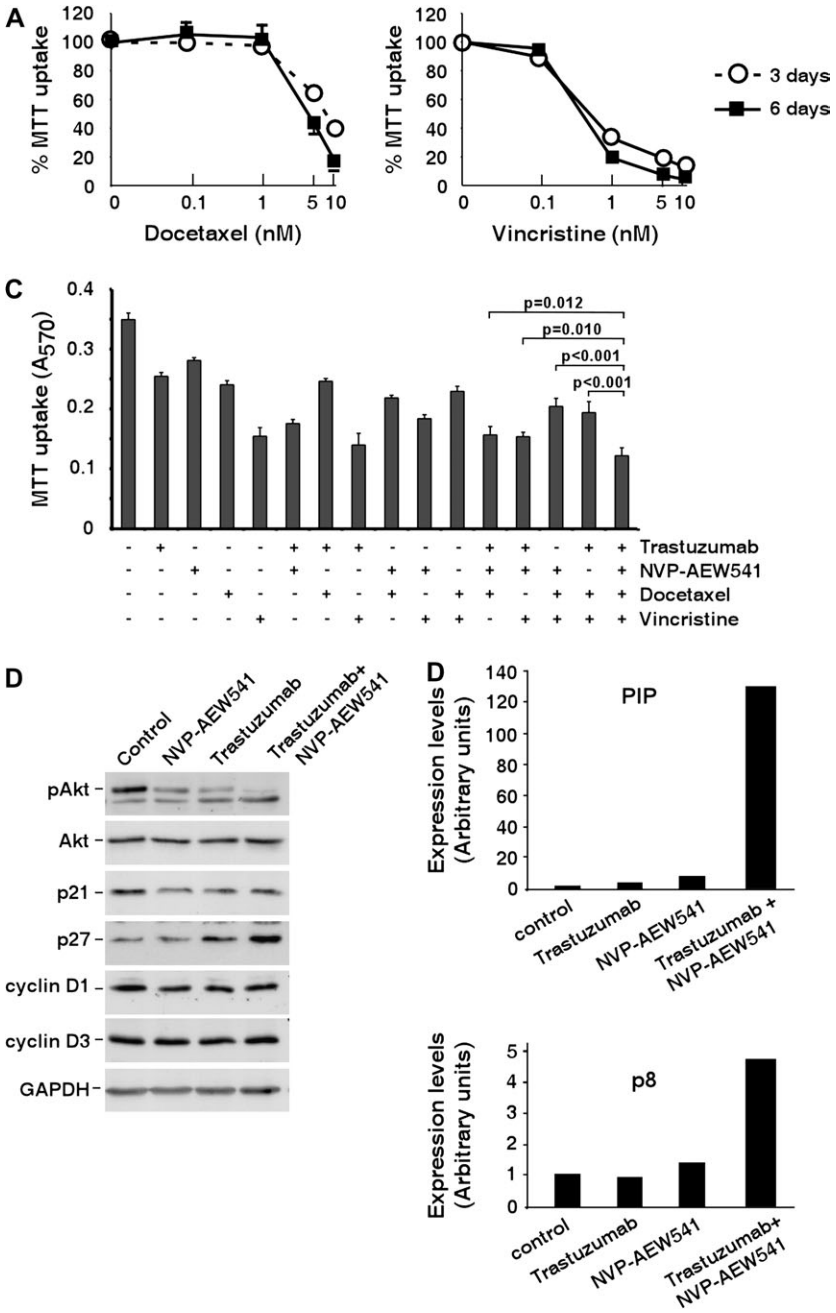

Figure 4. Combination of NVP-AEW541 with other antitumoral agents. (A) Action of docetaxel or vincristine on BT474 cells. MTT assays were carried out as above. Graphics represent mean ± standard deviation of three experiments. (B) Effect of NVP-AEW541 (2 μM) in combination with trastuzumab (10 nM), docetaxel (5 nM), and/or vincristine (0.5 nM). MTT uptake was measured 3 days later. (C) Biochemical effects of trastuzumab (10 nM), NVP-AEW541 (2 μM), or the combination of both on several proteins of BT474 cells treated for 72 h with the indicated compounds. (D) Quantitative RT-PCR analyses of messenger RNAs for prolactin-induced protein or p8 in cells treated with trastuzumab (10 nM), NVP-AEW541 (2 μM), or the combination of both. The data shown are from one experiment, representative of two.

(MCF7), the HER2-overexpressing situation (BT474 and SKBR3), and the triple-negative, basal-like type of breast cancer, characterized by the absence of hormone and HER2 receptors (MDA-MB231). Of those here studied, the MCF7 cell line was the one that expressed the highest levels of IGF-IR and was also the most sensitive to NVP-AEW541. However, in musculoskeletal tumors other authors did not observe a correlation between the level of expression of the IGF-IR and the sensitivity to NVP-AEW541, even though correlation was found when analyzing the degree of tyrosine phosphorylation [22]. It is unlikely that the effect of NVP-AEW541 on breast cancer cells is due to nonspecific inhibition of other kinases. In fact, activation of HER2 by NRG was largely unaffected by doses of NVP-AEW541 as high as 10 μM, while activation of the IGF-IR was fully prevented at 1 μM (Esparís-Ogando A, unpublished observations).

Table 1. Genes differentially affected by the NVP-AEW541 and trastuzumab combination

Probe set	Accession	Gene	Fold change
206509_at	NM_002652	Prolactin-induced protein	11.49
204607_at	NM_005518	3-Hydroxy-3-methylglutaryl-coenzyme A synthase 2 (mitochondrial)	5.53
205513_at	NM_001062	Transcobalamin I (vitamin B12-binding protein)	5.27
206799_at	NM_006551	Secretoglobin, family 1D, member 2	5.01
215492_x_at	AL035587	Pre-T-cell antigen receptor alpha	4.9
205319_at	NM_005672	Prostate stem-cell antigen	3.93
1562821_a_at	AF401033	M41 mRNA, complete sequence; alternatively spliced	3.81
206224_at	NM_001898	Cystatin SN	3.56
203504_s_at	NM_005502	ATP-binding cassette, subfamily A (ABC1), member 1	3.54
209813_x_at	M16768	T-cell receptor gamma constant 2	3.33
224146_s_at	AF352582	ATP-binding cassette transporter subfamily C member 11/Multidrug resistance associated Protein 8	3.28
209185_s_at	AF073310	Insulin receptor substrate 2	3.1
202833_s_at	NM_000295	Serine (or cysteine) proteinase inhibitor (alpha-1 antiproteinase, antitrypsin), member 1	3.07
201884_at	NM_004363	Carcinoembryonic antigen-related cell adhesion molecule 5	2.98
38707_r_at	S75174	E2F transcription factor 4, p107/p130 binding	2.9
228210_at	T10030	Neurexophilin 3	2.86
229441_at	AI569872	Protease, serine, 23	2.79
243313_at	AI141151	Synaptopodin 2-like	2.75
205697_at	NM_006998	Secretagogin, EF-hand calcium-binding protein	2.74
211144_x_at	M30894	T-cell receptor gamma constant 2	2.74
213106_at	AI769688	ATPase, aminophospholipid transporter, class I, type 8A, member 1	2.73
209460_at	AF237813	4-Aminobutyrate aminotransferase	2.72
227145_at	AW190565	Lysyl oxidase-like 4	2.65
211429_s_at	AF119873	Serine (or cysteine) proteinase inhibitor (alpha-1 antiproteinase, antitrypsin), member 1	2.64
212646_at	D42043	Raft-linking protein	2.64
228081_at	BF061444	Cyclin G2	2.62
208555_x_at	NM_001322	Cystatin SA	2.59
238476_at	AA481560	Adult retina protein	2.56
222453_at	AL136693	Cytochrome b reductase 1	2.54
205749_at	NM_000499	Cytochrome P450, family 1, subfamily A, polypeptide 1	2.53
226279_at	AW471145	Protease, serine, 23	2.44
202488_s_at	NM_005971	FXYD domain-containing ion transport regulator 3	2.37
206994_at	NM_001899	Cystatin S	2.3
203029_s_at	NM_002847	Protein tyrosine phosphatase, receptor type, N polypeptide 2	2.29
200742_s_at	BG231932	Tripeptidyl peptidase I	2.23
201009_s_at	AI439556	Thioredoxin interacting protein	2.23
202793_at	NM_005768	Putative protein similar to nessy (Drosophila)	2.23
204567_s_at	NM_004915	ATP-binding cassette, subfamily G (WHITE), member 1	2.22
201525_at	NM_001647	Apolipoprotein D	2.2
219440_at	NM_021785	Retinoic acid-induced 2	2.19
225664_at	AA788946	Collagen, type XII, alpha 1	2.18
208791_at	M25915	Clusterin	2.17
209230_s_at	AF135266	p8 protein (candidate of metastasis 1)	2.17
220177_s_at	NM_024022	Transmembrane protease, serine 3	2.17
206772_at	NM_005048	Parathyroid hormone receptor 2	−2.13
242138_at	BF060783	Distal-less homeobox 1	−2.2
205081_at	NM_001311	Cysteine-rich protein 1 (intestinal)	−2.26
226350_at	AU155565	Choroideremia-like (Rab escort protein 2)	−2.27
204913_s_at	AI360875	Sex determining region Y (SRY)-box 11	−2.28
219990_at	NM_024680	FLJ23311 protein	−2.3
228577_x_at	AI338465	KIAA1229 protein	−2.31
212983_at	NM_005343	v-Ha-ras Harvey rat sarcoma viral oncogene homolog	−2.32
1568764_x_at	AI692169	Programmed cell death 6	−2.33
209308_s_at	BC002461	BCL2/adenovirus E1B 19 kDa interacting protein 2	−2.34
214595_at	AI332979	Potassium voltage-gated channel, subfamily G, member 1	−2.35
231747_at	NM_006639	Cysteinyl leukotriene receptor 1	−2.35
211812_s_at	AB050856	UDP-Gal:betaGlcNAc beta 1,3-galactosyltransferase, polypeptide 3	−2.36

Table 1. (*Continued*)

Probe set	Accession	Gene	Fold change
1554614_a_at	AB051233	Polypyrimidine tract-binding protein 2	−2.4
224100_s_at	BC002874	Dihydropyrimidinase-like 5	−2.4
219742_at	NM_030567	Proline-rich 7 (synaptic)	−2.42
242939_at	AI950069	Transcription factor Dp-1	−2.43
212224_at	NM_000689	Aldehyde dehydrogenase 1 family, member A1	−2.62
225612_s_at	BE672260	UDP-GlcNAc:betaGal beta-1,3-*N*-acetylglucosaminyltransferase 5	−2.62
227405_s_at	AW340311	Frizzled homolog 8 (Drosophila)	−2.66
230472_at	AI870306	Iroquois homeobox protein 1	−2.81
221586_s_at	U15642	E2F transcription factor 5, p130 binding	−2.84
221606_s_at	BC005342	Nucleosomal-binding protein 1	−2.9
219737_s_at	AI524125	Protocadherin 9	−2.93
226611_s_at	AA722878	Proline-rich 6	−2.97
202856_s_at	NM_004207	Solute carrier family 16 (monocarboxylic acid transporters), member 3	−2.98
226931_at	AU151239	ARG99 protein	−3.01
207030_s_at	NM_001321	Cysteine- and glycine-rich protein 2	−3.1
212298_at	BE620457	Neuropilin 1	−3.16
232010_at	AA129444	Follistatin-like 5	−3.44
206793_at	NM_002686	Phenylethanolamine *N*-methyltransferase	−3.49
203434_s_at	AI433463	Membrane metalloendopeptidase (CALLA, CD10)	−3.8
242301_at	R60224	Cerebellin 2 precursor	−4.1
1569729_a_at	BC034963	Ankyrin repeat, SAM and basic leucine zipper domain containing 1	−4.69
228038_at	AI669815	SRY-box 2	−7.01
210933_s_at	BC004908	Fascin homolog 1, actin-bundling protein (*Strongylocentrotus purpuratus*)	−9.08

BT474 cells were treated with NVP-AEW541, trastuzumab, or NVP-AEW541 and trastuzumab combination, and messenger RNAs (mRNAs) were isolated and analyzed for expression as described under the 'Materials and Methods' section. Genes affected by the NVP-AEW541 and trastuzumab combination are described as the fold change (mean from two different experiments carried out in duplicate) with respect to untreated BT474 cells. Genes whose changes using the combination were identical to those found upon individual treatments with either trastuzumab or NVP-AEW541 have not been included. ATP, adenosine triphosphate.

Interestingly, expression of activated pIGF-IR was observed under resting conditions. Although the reason for such an activation has not been explored, resting IGF-IR activation may be due to IGF-I availability, either produced autocrinally or supplied by serum. The mechanism of action of NVP-AEW541 on breast cancer cells is complex and involves cell cycle arrest and apoptosis. NVP-AEW541 induced an increase in the G_0/G_1 and a decrease in S phase, and biochemical studies demonstrated that this effect may be due to an increase in p27 levels. These findings are in line with other reports that have shown that IGF-IR-transfected cells express lower levels of p27 [11]. The increase in p27 levels could be secondary to Akt inactivation, as this kinase plays a predominant role in regulating p27 stability and subcellular distribution [33]. Analogous decreases in pAkt levels have been described in neuroblastoma or sarcoma cells treated with NVP-AEW541 [22, 23]. By contrast, NVP-AEW541 produced a decrease in p21. This finding may in principle result paradoxical due to the proposed role of p21 as a negative regulator of cell cycle progression [34]. However, previous observations indicate that up-regulation of p21 is required for IGF-IR-induced proliferation in MCF7 cells [35].

We also observed an increase in Annexin V staining and a decrease in the mitochondrial membrane potential, both signs of apoptotic cell death. The changes in the mitochondrial membrane potential were detected at high doses of NVP-AEW541. Although the degree of induction of Annexin V staining was low and only observed at high concentrations of the drug, our results indicate that apoptotic cell death may play a role in the action of NVP-AEW541 on breast cancer cells. Indeed, a recent report in myeloid leukemia cells has shown that NVP-AEW541 induces apoptosis as the principal mechanism of action [36]. In a similar manner, other anti-IGF-IR strategies such as monoclonal antibodies have shown to produce a proapoptotic effect which was partially attributed to alterations in the ratio of proapoptotic and anti-apoptotic (Bax/Bcl-2) proteins [37].

High expression of IGF-IR in breast cancer cells has been linked to trastuzumab resistance [11]. This opens the interesting possibility of using therapies that target IGF-IR to favor responses to trastuzumab. Following this reasoning, we studied the anti-proliferative effect of both drugs administered in combination. Addition of NVP-AEW541 and trastuzumab was synergistic, and this occurred in the trastuzumab-sensitive cell lines BT474 and SKBR3, but not in trastuzumab-resistant MCF7 cells. In contrast, combination of NVP-AEW541 with other agents commonly used in the breast cancer clinic, such as docetaxel or vincristine, was not effective in terms of potentiation. Interestingly, the combination of NVP-AEW541 and trastuzumab produced the same anti-proliferative effect than the combination of trastuzumab and docetaxel. It is important to mention that the combination of trastuzumab

and taxanes is one of the gold standards in the treatment of breast cancer patients with HER2-overexpressing tumors [38]. In addition to our findings, precedents of increased action of trastuzumab when combined with anti-IGF-IR antibodies or IGF-I-binding proteins indicate that the combination of trastuzumab with anti-IGF-IR agents is active and could be further explored in phase Ib-II clinical trials. Furthermore, the potential combination of anti-IGF-IR antagonists with lapatinib (a dual epidermal growth factor receptor and HER2 inhibitor that is reaching the breast cancer clinic) may prevent the discomfort and expenses of drugs that require parenteral administration.

With respect to the mechanism of potentiation of the action of trastuzumab by NVP-AEW541, biochemical studies indicated that the combination of both drugs exerted a higher effect on the levels of pAkt and p27 than either drug administered alone. Given the importance of p27 as a mediator of the action of trastuzumab on breast cancer cells overexpressing HER2 [39, 40], it is possible that changes in the levels of p27 may play a role in the action of the combined treatment on these cells. In addition to these data, genomic studies identified several genes whose mRNAs were modified by the combined treatment. Among them, the PIP appeared to be the most highly up-regulated. Although its function in the mammary gland is unknown, PIP has been reported to be a small glycoprotein secreted by breast carcinomas [41, 42]. Another interesting finding was the profound effect of the combination on the actin-bundling protein fascin homolog 1 protein mRNA levels. This protein organizes filamentous actin into bundles present in microspikes, membrane ruffles, and stress fibers. Fascin homolog 1 has been reported to be overexpressed in breast cancer, and increased levels of the protein correlate with a poor prognosis [43]. In addition, p8, a small protein involved in stress-induced apoptotic cell death, was also up-regulated by the combined treatment [30]. Other genes that participate in cell cycle progression through binding to p130 and the control of RB function, such as E2F-4, E2F-5, or TFDP1 (which also may control apoptosis), were also specifically modified by the combined treatment. Interestingly, several proteins involved in the control of proteolytic processes were also modified by the combined treatment. Of these, several cystatins were up-regulated. Cystatins S, SN, and SA are secreted proteins that inhibit the function of cysteine proteases. The Cystatins have been reported to control multiple processes, involving cell proliferation or apoptosis, and may be useful antitumoral agents [44]. Taken together, the biochemical and genomic data indicate that the combination of trastuzumab and NVP-AEW541 may exert its action on breast cancer cells through a complex array of transcriptional and posttranscriptional modifications of proteins that control cell number.

The findings of our study have important clinical implications. We confirm that the IGF-IR is frequently overexpressed in breast tumors and that targeting of this receptor affects proliferation and survival of breast cancer cells. Although others have used anti-IGF-IR antibodies to achieve an analogous effect, these antibodies may also inhibit the insulin receptor provoking metabolic disorders [19]. It is therefore important to search for alternative ways to decrease IGF-IR activity, and in this respect, the use of specific tyrosine kinase inhibitors could overcome this problem. We further observed that the inhibition of two tyrosine kinase receptors, the IGF-IR and HER2, increases the anti-proliferative activity when compared with the effect of targeting either receptor alone, indicating that this approach should be explored in the design of clinical studies. Furthermore, the combination of these both drugs was much more active than the combination of therapeutic strategies that are currently the standard of care, as is the case of trastuzumab plus docetaxel. In summary, our results support the clinical development of anti-IGF-IR agents in breast cancer, especially in combination with agents, such as trastuzumab, that target HER2.

funding

Ministry of Science and Technology of Spain (BFU2006-01813/BMC to A.P.); Scientific Foundation of the Spanish Association for Cancer Research (AECC); Instituto de Salud Carlos III (PI061552 and CP04/00045 to A.E.O.); Spanish Cancer Centers Network Program (RD06/0020/0041); European Community through the regional development funding program (FEDER) to Cancer Research Institute.

acknowledgements

We wish to thank Dr Johan Zimmerman (Novartis Pharma, Basel, Switzerland) for comments on the manuscript and Dr Mark Andrew Pearson (Novartis Pharma) for initially providing NVP-AEW541.

references

1. Blume-Jensen P, Hunter T. Oncogenic kinase signalling. Nature 2001; 411: 355–365.
2. Hynes NE, Lane HA. ERBB receptors and cancer: the complexity of targeted inhibitors. Nat Rev Cancer 2005; 5: 341–354.
3. Nahta R, Yu D, Hung MC et al. Mechanisms of disease: understanding resistance to HER2-targeted therapy in human breast cancer. Nat Clin Pract Oncol 2006; 3: 269–280.
4. Slamon DJ, Clark GM, Wong SG et al. Human breast cancer: correlation of relapse and survival with amplification of the HER-2/neu oncogene. Science 1987; 235: 177–182.
5. Nahta R, Esteva FJ. Trastuzumab: triumphs and tribulations. Oncogene 2007; 26: 3637–3643.
6. Yarden Y, Sliwkowski MX. Untangling the ErbB signalling network. Nat Rev Mol Cell Biol 2001; 2: 127–137.
7. Slamon DJ, Leyland-Jones B, Shak S et al. Use of chemotherapy plus a monoclonal antibody against HER2 for metastatic breast cancer that overexpresses HER2. N Engl J Med 2001; 344: 783–792.
8. Baselga J, Perez EA, Pienkowski T, Bell R. Adjuvant trastuzumab: a milestone in the treatment of HER-2-positive early breast cancer. Oncologist 2006; 11(Suppl 1): 4–12.
9. Nagata Y, Lan KH, Zhou X et al. PTEN activation contributes to tumor inhibition by trastuzumab, and loss of PTEN predicts trastuzumab resistance in patients. Cancer Cell 2004; 6: 117–127.
10. Scaltriti M, Rojo F, Ocana A et al. Expression of p95HER2, a truncated form of the HER2 receptor, and response to anti-HER2 therapies in breast cancer. J Natl Cancer Inst 2007; 99: 628–638.

11. Lu Y, Zi X, Zhao Y et al. Insulin-like growth factor-I receptor signaling and resistance to trastuzumab (Herceptin). J Natl Cancer Inst 2001; 93: 1852–1857.
12. Ibrahim YH, Yee D. Insulin-like growth factor-I and breast cancer therapy. Clin Cancer Res 2005; 11: 944s–950s.
13. Surmacz E. Function of the IGF-I receptor in breast cancer. J Mammary Gland Biol Neoplasia 2000; 5: 95–105.
14. Hankinson SE, Willett WC, Colditz GA et al. Circulating concentrations of insulin-like growth factor-I and risk of breast cancer. Lancet 1998; 351: 1393–1396.
15. Jerome L, Shiry L, Leyland-Jones B. Deregulation of the IGF axis in cancer: epidemiological evidence and potential therapeutic interventions. Endocr Relat Cancer 2003; 10: 561–578.
16. Carboni JM, Lee AV, Hadsell DL et al. Tumor development by transgenic expression of a constitutively active insulin-like growth factor I receptor. Cancer Res 2005; 65: 3781–3787.
17. Hartog H, Wesseling J, Boezen HM, van der Graaf WT. The insulin-like growth factor 1 receptor in cancer: old focus, new future. Eur J Cancer 2007; 43: 1895–1904.
18. Haluska P, Shaw HM, Batzel GN et al. Phase I dose escalation study of the anti insulin-like growth factor-I receptor monoclonal antibody CP-751,871 in patients with refractory solid tumors. Clin Cancer Res 2007; 13: 5834–5840.
19. Sachdev D, Singh R, Fujita-Yamaguchi Y, Yee D. Down-regulation of insulin receptor by antibodies against the type I insulin-like growth factor receptor: implications for anti-insulin-like growth factor therapy in breast cancer. Cancer Res 2006; 66: 2391–2402.
20. Garcia-Echeverria C, Pearson MA, Marti A et al. In vivo antitumor activity of NVP-AEW541-A novel, potent, and selective inhibitor of the IGF-IR kinase. Cancer Cell 2004; 5: 231–239.
21. Mitsiades CS, Mitsiades NS, McMullan CJ et al. Inhibition of the insulin-like growth factor receptor-1 tyrosine kinase activity as a therapeutic strategy for multiple myeloma, other hematologic malignancies, and solid tumors. Cancer Cell 2004; 5: 221–230.
22. Scotlandi K, Manara MC, Nicoletti G et al. Antitumor activity of the insulin-like growth factor-I receptor kinase inhibitor NVP-AEW541 in musculoskeletal tumors. Cancer Res 2005; 65: 3868–3876.
23. Tanno B, Mancini C, Vitali R et al. Down-regulation of insulin-like growth factor I receptor activity by NVP-AEW541 has an antitumor effect on neuroblastoma cells in vitro and in vivo. Clin Cancer Res 2006; 12: 6772–6780.
24. Cabrera N, Díaz-Rodríguez E, Becker E et al. TrkA receptor ectodomain cleavage generates a tyrosine-phosphorylated cell-associated fragment. J Cell Biol 1996; 132: 427–436.
25. Esparís-Ogando A, Diaz-Rodriguez E, Montero JC et al. Erk5 participates in neuregulin signal transduction and is constitutively active in breast cancer cells overexpressing ErbB2. Mol Cell Biol 2002; 22: 270–285.
26. Chou TC, Motzer RJ, Tong Y, Bosl GJ. Computerized quantitation of synergism and antagonism of taxol, topotecan, and cisplatin against human teratocarcinoma cell growth: a rational approach to clinical protocol design. J Natl Cancer Inst 1994; 86: 1517–1524.
27. Agus D, Akita R, Fox W et al. Targeting ligand-activated ErbB2 signaling inhibits breast and prostate tumor growth. Cancer Cell 2002; 2: 127–137.
28. Finn RS, Dering J, Ginther C et al. Dasatinib, an orally active small molecule inhibitor of both the src and abl kinases, selectively inhibits growth of basal-type/''triple-negative'' breast cancer cell lines growing in vitro. Breast Cancer Res Treat 2007; 105(3): 319–326.
29. Yuste L, Montero JC, Esparis-Ogando A, Pandiella A. Activation of ErbB2 by overexpression or by transmembrane neuregulin results in differential signaling and sensitivity to herceptin. Cancer Res 2005; 65: 6801–6810.
30. Carracedo A, Lorente M, Egia A et al. The stress-regulated protein p8 mediates cannabinoid-induced apoptosis of tumor cells. Cancer Cell 2006; 9: 301–312.
31. Jerome L, Alami N, Belanger S et al. Recombinant human insulin-like growth factor binding protein 3 inhibits growth of human epidermal growth factor receptor-2-overexpressing breast tumors and potentiates herceptin activity in vivo. Cancer Res 2006; 66: 7245–7252.
32. Nahta R, Yuan LX, Zhang B et al. Insulin-like growth factor-I receptor/human epidermal growth factor receptor 2 heterodimerization contributes to trastuzumab resistance of breast cancer cells. Cancer Res 2005; 65: 11118–11128.
33. Shin I, Yakes FM, Rojo F et al. PKB/Akt mediates cell-cycle progression by phosphorylation of p27(Kip1) at threonine 157 and modulation of its cellular localization. Nat Med 2002; 8: 1145–1152.
34. Weiss RH. p21(Waf1/Cip1) as a therapeutic target in breast and other cancers. Cancer Cell 2003; 4: 425–429.
35. Dupont J, Karas M, LeRoith D. The cyclin-dependent kinase inhibitor p21CIP/WAF is a positive regulator of insulin-like growth factor I-induced cell proliferation in MCF-7 human breast cancer cells. J Biol Chem 2003; 278: 37256–37264.
36. Tazzari PL, Tabellini G, Bortul R et al. The insulin-like growth factor-I receptor kinase inhibitor NVP-AEW541 induces apoptosis in acute myeloid leukemia cells exhibiting autocrine insulin-like growth factor-I secretion. Leukemia 2007; 21(5): 886–896.
37. Butt AJ, Firth SM, King MA, Baxter RC. Insulin-like growth factor-binding protein-3 modulates expression of Bax and Bcl-2 and potentiates p53-independent radiation-induced apoptosis in human breast cancer cells. J Biol Chem 2000; 275: 39174–39181.
38. Esteva FJ, Valero V, Booser D et al. Phase II study of weekly docetaxel and trastuzumab for patients with HER-2-overexpressing metastatic breast cancer. J Clin Oncol 2002; 20: 1800–1808.
39. Yakes FM, Chinratanalab W, Ritter CA et al. Herceptin-induced inhibition of phosphatidylinositol-3 kinase and Akt is required for antibody-mediated effects on p27, cyclin D1, and antitumor action. Cancer Res 2002; 62: 4132–4141.
40. Lane HA, Beuvink I, Motoyama AB et al. ErbB2 potentiates breast tumor proliferation through modulation of p27(Kip1)-Cdk2 complex formation: receptor overexpression does not determine growth dependency. Mol Cell Biol 2000; 20: 3210–3223.
41. Basmaciogullari S, Autiero M, Culerrier R et al. Mapping the CD4 binding domain of gp17, a glycoprotein secreted from seminal vesicles and breast carcinomas. Biochemistry 2000; 39: 5332–5340.
42. Caputo E, Manco G, Mandrich L, Guardiola J. A novel aspartyl proteinase from apocrine epithelia and breast tumors. J Biol Chem 2000; 275: 7935–7941.
43. Yoder BJ, Tso E, Skacel M et al. The expression of fascin, an actin-bundling motility protein, correlates with hormone receptor-negative breast cancer and a more aggressive clinical course. Clin Cancer Res 2005; 11: 186–192.
44. Keppler D. Towards novel anti-cancer strategies based on cystatin function. Cancer Lett 2006; 235: 159–176.